Electronic Supplementary Material (ESI) for CrystEngComm.

Supplementary information

Lactic-acid enhanced solvothermal crystallization, color-tunable photoluminescence, and thermal stability of h-$LaPO_4$:Ce^{3+},Tb^{3+},Sm^{3+} nanocrystals

Junfeng Zou,[a] Qi Zhu,[a] Ji-Guang Li*[b]

[a] *Key Laboratory for Anisotropy and Texture of Materials (Ministry of Education), School of Materials Science and Engineering, Northeastern University, Shenyang, Liaoning 110819, China*

[b] *Research Center for Functional Materials, National Institute for Materials Science, Namiki 1-1, Tsukuba, Ibaraki 305-0044, Japan*

*Corresponding author

Dr. Ji-Guang Li

National Institute for Materials Science

Tel: +81-29-860-4394

E-mail: li.jiguang@nims.go.jp

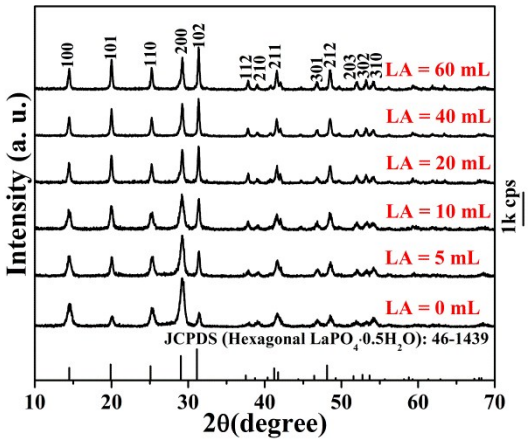

Fig. S1. XRD patterns for the h-$(La_{0.90}Ce_{0.05}Tb_{0.05})PO_4$ samples synthesized with different LA contents.

Table S1. Intensity ratio *R* of (102) to (200) diffractions and crystallite size for the h-$(La_{0.90}Ce_{0.05}Tb_{0.05})PO_4$ samples as a function of LA content.

LA content (mL)	0	5	10	20	40	60
Intensity ratio (*R*)	0.30	0.62	0.88	1.10	1.15	1.31
Crystallite size/nm	19.0	21.9	26.1	29.2	30.6	32.8

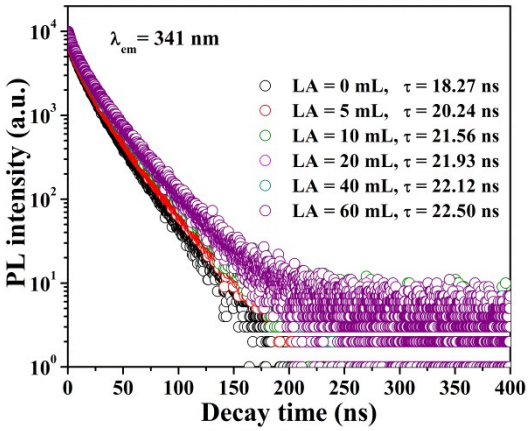

Fig. S2. Fluorescence decay curves for the 341 nm emission of Ce^{3+} in the h-$(La_{0.90}Ce_{0.05}Tb_{0.05})PO_4$ samples synthesized with different LA contents.

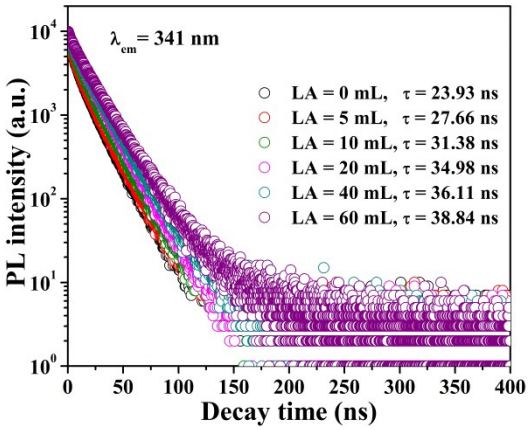

Fig. S3. Fluorescence decay curves for the 341 nm emission of Ce^{3+} in the h-$(La_{0.95}Ce_{0.05})PO_4$ samples synthesized with different LA contents.

Table S2. Results of second-order exponential fitting for the 341 nm fluorescence decay of Ce^{3+} in the h-($La_{0.90}Ce_{0.05}Tb_{0.05}$)$PO_4$ samples synthesized with different LA contents.

LA content/mL	A_1	τ_1/ns	A_2	τ_2/ns	R^2	τ^*/ns
0	5181.90	7.49	3899.83	22.95	0.99643	18.27
5	5253.60	8.06	4153.51	25.17	0.99627	20.24
10	5301.41	8.44	4322.63	26.66	0.99616	21.56
20	5227.40	8.65	4308.77	27.08	0.99681	21.93
40	5190.39	8.75	4301.83	27.29	0.99701	22.12
60	5116.39	8.96	4287.97	27.72	0.99644	22.50

Table S3. Results of second-order exponential fitting for the 341 nm fluorescence decay of Ce^{3+} in the h-($La_{0.95}Ce_{0.05}$)PO_4 samples synthesized with different LA contents.

LA content/mL	A_1	τ_1/ns	A_2	τ_2/ns	R^2	τ^*/ns
0	4722.35	9.27	4642.61	28.74	0.99726	23.93
5	4722.14	14.41	4645.50	33.46	0.99794	27.66
10	4721.94	19.03	4648.10	37.71	0.99855	31.38
20	4721.81	22.12	4649.84	40.55	0.99895	33.98
40	5872.80	25.52	3464.96	46.06	0.99791	36.11
60	5088.49	25.18	4416.74	47.23	0.99686	38.84

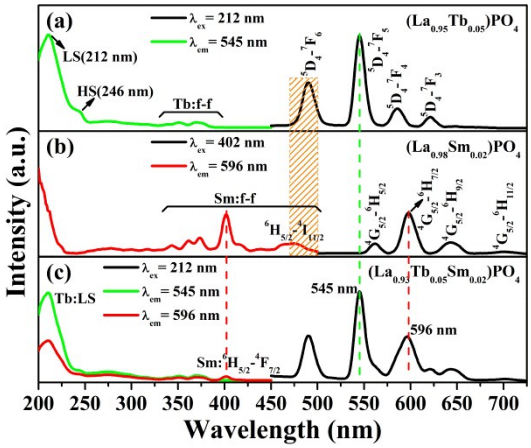

Fig. S4. PLE and PL spectra of the ($La_{0.95}Tb_{0.05}$)PO_4 (a), ($La_{0.98}Sm_{0.02}$)PO_4 (b), and ($La_{0.93}Tb_{0.05}Sm_{0.02}$)$PO_4$ (c) samples.

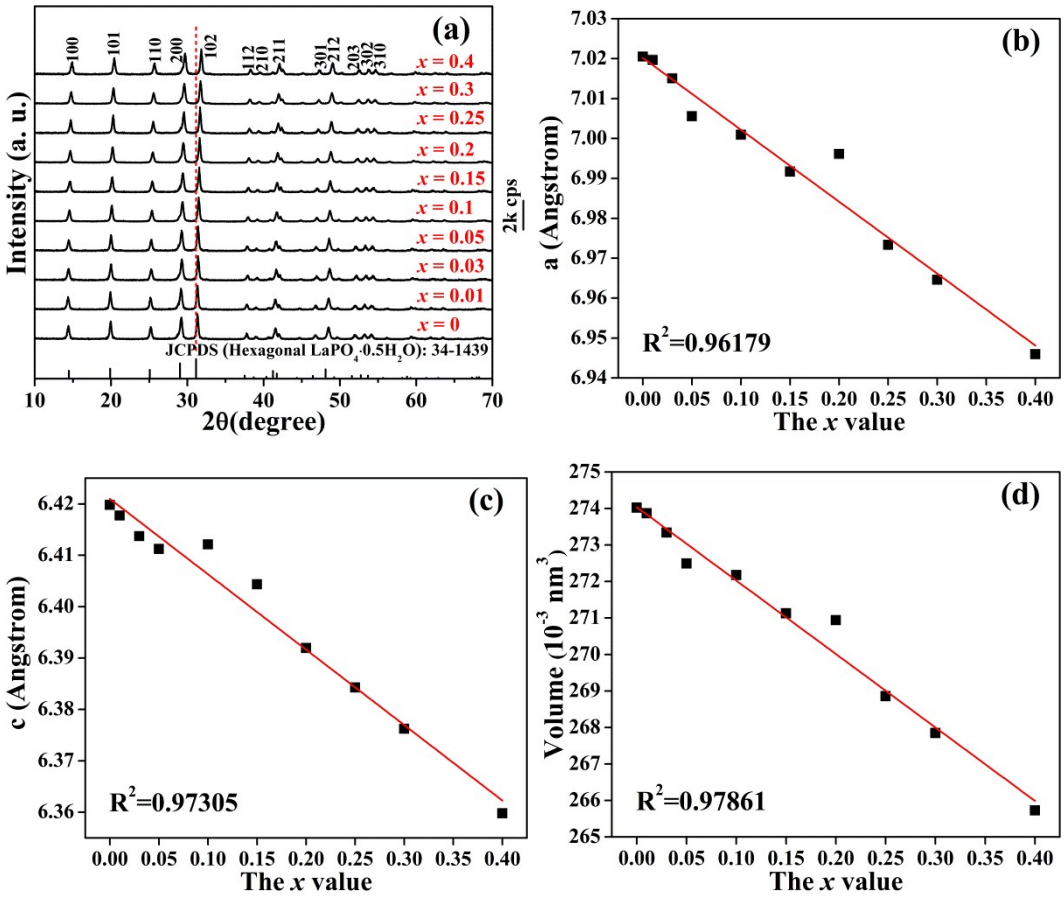

Fig. S5. XRD patterns (a) and the correlation of lattice parameters *a*/*b* (b, *a*=*b*) and *c* (c) and cell volume *V* (d) with the Tb^{3+} content for the h-$(La_{0.93-x}Ce_{0.05}Tb_xSm_{0.02})PO_4$ samples (x = 0-0.40).

Table S4. Results of second-order exponential fitting for the 341 nm fluorescence decay of Ce^{3+} in the $(La_{0.93-x}Ce_{0.05}Tb_xSm_{0.02})PO_4$ (x = 0-0.40) samples.

x value	A_1	τ_1/ns	A_2	τ_2/ns	R^2	τ^*/ns
0	5831.13	5.58	3018.16	20.05	0.99561	14.99
0.01	6390.39	4.51	2545.65	17.97	0.99342	12.77
0.03	6143.96	3.47	1908.58	18.33	0.97398	12.70
0.05	6677.28	3.76	2181.28	15.87	0.99233	10.78
0.10	6858.91	3.11	1995.68	14.49	0.99123	9.66
0.15	7526.94	2.56	1947.59	12.48	0.99096	8.09
0.20	7394.11	2.52	1828.04	12.32	0.98932	7.88
0.25	7884.39	1.94	1806.01	9.43	0.99480	5.89
0.30	7682.61	1.60	1821.50	8.51	0.99315	5.45
0.40	8653.81	1.67	1285.52	8.67	0.99370	4.72

Table S5. Results of single exponential fitting for the 545 nm fluorescence decay of Tb^{3+} in the $(La_{0.93-x}Ce_{0.05}Tb_xSm_{0.02})PO_4$ (x = 0.01-0.40) samples.

x value	A	R^2	τ/ms
0.01	9913.83	0.99947	1.89
0.03	3438.98	0.99819	3.15
0.05	4504.22	0.99983	4.41
0.10	7105.47	0.99953	3.58
0.15	7481.19	0.99908	3.17
0.20	8511.86	0.99846	2.82
0.25	8529.36	0.99668	2.35
0.30	9940.90	0.99499	2.07

0.40	6826.29	0.98837	1.71

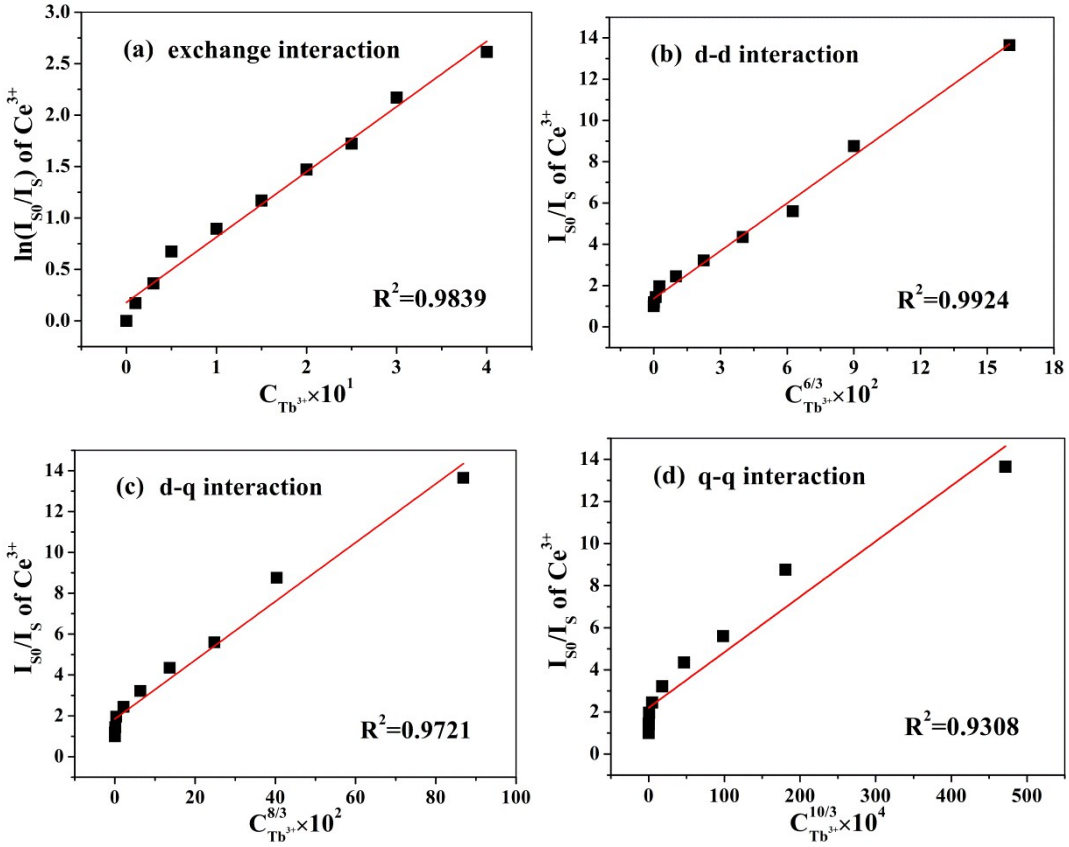

Fig. S6. Dependence of $\ln(I_{S0}/I_S)$ on C (a) and (I_{S0}/I_S) on $C^{6/3}$ (b), $C^{8/3}$ (c), and $C^{10/3}$ (d) for Ce^{3+} emission in the $(La_{0.93-x}Ce_{0.05}Tb_xSm_{0.02})PO_4$ (x = 0-0.40) samples.

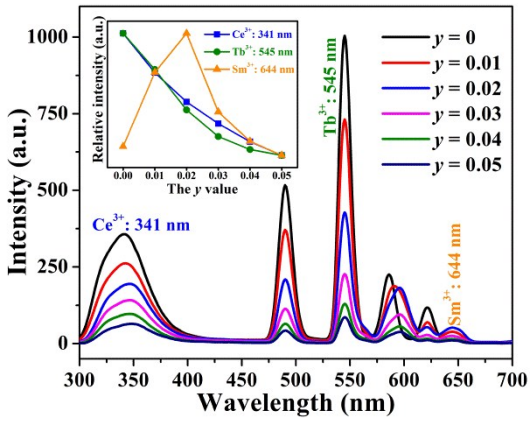

Fig. S7. PL spectra of the $(La_{0.75-y}Ce_{0.05}Tb_{0.20}Sm_y)PO_4$ (y = 0-0.05) samples.

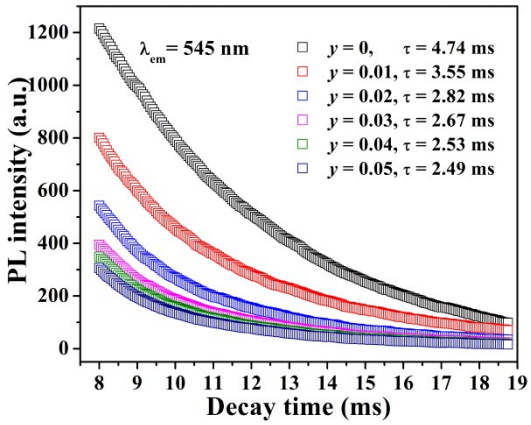

Fig. S8. Decay curves for the 545 nm emission of Tb^{3+} in the $(La_{0.75-y}Ce_{0.05}Tb_{0.20}Sm_y)PO_4$ (y = 0-0.05) samples.

Table S6. Results of single exponential fitting for the 545 nm fluorescence decay of Tb^{3+} in the $(La_{0.75-y}Ce_{0.05}Tb_{0.20}Sm_y)PO_4$ (y = 0-0.05) samples.

x value	A	R^2	τ/ms
0	6774.12	0.99990	4.74
0.01	7111.75	0.99951	3.55
0.02	8511.86	0.99846	2.82
0.03	7161.32	0.99786	2.67
0.04	7450.75	0.99739	2.53

0.05	6834.69	0.99732	2.49

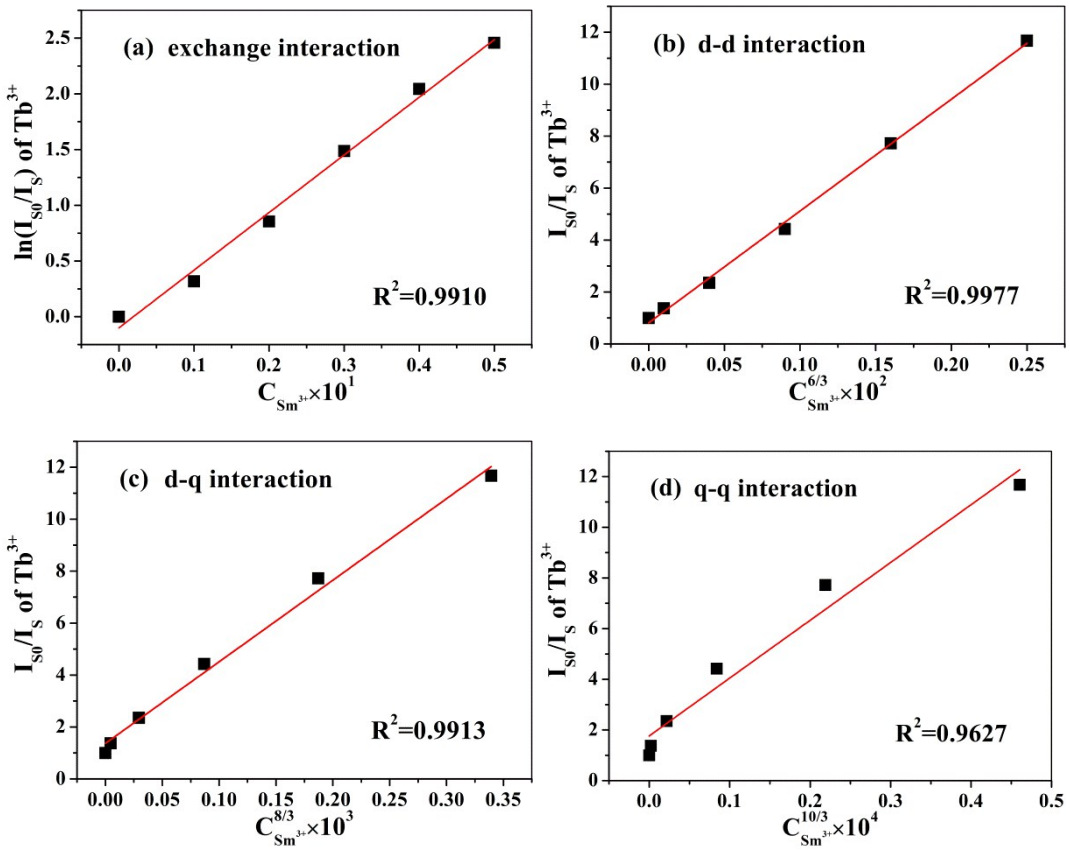

Fig. S9. Dependence of $\ln(I_{S0}/I_S)$ on C (a) and (I_{S0}/I_S) on $C^{6/3}$ (b), $C^{8/3}$ (c), and $C^{10/3}$ (d) for Tb^{3+} emission in the $(La_{0.75-y}Ce_{0.05}Tb_{0.20}Sm_y)PO_4$ (y = 0-0.05) samples.